

# Modulation of the electroluminescence emission from ZnO/Si NCs/p-Si light-emitting devices via pulsed excitation

J. López-Vidrier, S. Gutsch, O. Blázquez, D. Hiller, J. Laube, R. Kaur, S. Hernández, B. Garrido, and M. Zacharias

Citation: *Appl. Phys. Lett.* **110**, 203104 (2017); doi: 10.1063/1.4983722

View online: <https://doi.org/10.1063/1.4983722>

View Table of Contents: <http://aip.scitation.org/toc/apl/110/20>

Published by the [American Institute of Physics](#)

---

## Articles you may be interested in

[Tunnel-injected sub-260 nm ultraviolet light emitting diodes](#)  
Applied Physics Letters **110**, 201102 (2017); 10.1063/1.4983352

[Chemical etching of silicon carbide in pure water by using platinum catalyst](#)  
Applied Physics Letters **110**, 201601 (2017); 10.1063/1.4983206

[Electrically driven terahertz radiation of 2DEG plasmons in AlGaIn/GaN structures at 110 K temperature](#)  
Applied Physics Letters **110**, 202101 (2017); 10.1063/1.4983286

[Influence of metal choice on \(010\)  \$\beta\$ -Ga<sub>2</sub>O<sub>3</sub> Schottky diode properties](#)  
Applied Physics Letters **110**, 202102 (2017); 10.1063/1.4983610

[Gallium vacancies in  \$\beta\$ -Ga<sub>2</sub>O<sub>3</sub> crystals](#)  
Applied Physics Letters **110**, 202104 (2017); 10.1063/1.4983814

[The effect of device electrode geometry on performance after hot-carrier stress in amorphous In-Ga-Zn-O thin film transistors with different via-contact structures](#)  
Applied Physics Letters **110**, 202103 (2017); 10.1063/1.4983713

---



**THE WORLD'S RESOURCE FOR  
VARIABLE TEMPERATURE  
SOLID STATE CHARACTERIZATION**



OPTICAL STUDIES SYSTEMS



SEEBECK STUDIES SYSTEMS



MICROPROBE STATIONS



HALL EFFECT STUDY SYSTEMS AND MAGNETS

[WWW.MMR-TECH.COM](http://WWW.MMR-TECH.COM)

## Modulation of the electroluminescence emission from ZnO/Si NCs/*p*-Si light-emitting devices via pulsed excitation

J. López-Vidrier,<sup>1,a)</sup> S. Gutsch,<sup>1</sup> O. Blázquez,<sup>2</sup> D. Hiller,<sup>1</sup> J. Laube,<sup>1</sup> R. Kaur,<sup>1</sup> S. Hernández,<sup>2</sup> B. Garrido,<sup>2</sup> and M. Zacharias<sup>1</sup>

<sup>1</sup>Laboratory for Nanotechnology, IMTEK, Faculty of Engineering, University of Freiburg, Georges Köhler Allee 103, D-79110 Freiburg, Germany

<sup>2</sup>Departament d'Enginyeries: Electrònica, MIND-IN<sup>2</sup>UB, Universitat de Barcelona, Martí i Franquès 1, E-08028 Barcelona, Spain

(Received 31 March 2017; accepted 5 May 2017; published online 19 May 2017)

In this work, the electroluminescence (EL) emission of zinc oxide (ZnO)/Si nanocrystals (NCs)-based light-emitting devices was studied under pulsed electrical excitation. Both Si NCs and deep-level ZnO defects were found to contribute to the observed EL. Symmetric square voltage pulses (50- $\mu$ s period) were found to notably enhance EL emission by about one order of magnitude. In addition, the control of the pulse parameters (accumulation and inversion times) was found to modify the emission lineshape, long inversion times (i.e., short accumulation times) suppressing ZnO defects contribution. The EL results were discussed in terms of the recombination dynamics taking place within the ZnO/Si NCs heterostructure, suggesting the excitation mechanism of the luminescent centers via a combination of electron impact, bipolar injection, and sequential carrier injection within their respective conduction regimes. *Published by AIP Publishing.*

[<http://dx.doi.org/10.1063/1.4983722>]

The potential of silicon nanocrystals (Si NCs) for optoelectronics has arisen the interest of the research community since the discovery of the quantum confinement effect,<sup>1</sup> which leads not only to a discretization of the allowed electronic states within the energy bands but also to an increase in the band gap energy of the bulk material.<sup>2,3</sup> In particular, the control of the NC size allows for Si band gap engineering,<sup>4</sup> which can be exploited towards tunable-light emission Si-based devices. For this reason, exhaustive efforts are dedicated to understand the charge injection mechanisms that yield electroluminescence (EL) emission from SiO<sub>2</sub>-embedded Si NCs-based light-emitting diodes (LEDs). Some reported works suggest bipolar injection to be the dominant excitation mechanism under DC conditions,<sup>5,6</sup> where simultaneous injection of electrons and holes into the NCs results in efficient exciton formation. Notwithstanding, the asymmetry of electrons and holes in tunneling through SiO<sub>2</sub> barriers often leads to a less efficient excitation via impact ionization.<sup>7,8</sup> To overcome limitations of DC excitation, pulsed emission was proposed that relies on the efficient sequential injection of electrons and holes into NCs,<sup>9–12</sup> effectively lowering operation voltages and hence increasing device stability.<sup>13</sup>

Considering the top contact, *n*-type poly-Si is typically employed for Si NC-based capacitors or field-effect transistors,<sup>5,6,9</sup> because it provides excellent charge injection and can be deposited and implanted via standard microelectronics techniques. Nevertheless, its absorption in the visible range overlaps with the Si NCs emission spectrum.<sup>14</sup> Therefore, wide-band gap *n*-type transparent conductive oxides (TCOs) such as indium tin oxide (ITO) are increasingly being used in these light-emitting systems.<sup>7,8</sup> In the present work, atomic

layer deposition (ALD) of zinc oxide (ZnO) was used for the top contact, which is a robust alternative for Si NCs-based LEDs.<sup>15,16</sup> In addition, ALD-ZnO presents luminescence properties under certain fabrication conditions and device design,<sup>16,17</sup> which could be used to complement the red-infrared NCs-based emission towards higher energies within the visible spectrum.

In this work, devices containing Si NCs/SiO<sub>2</sub> multilayers (MLs) as active luminescent layer were employed. A total number of five SiO<sub>0.93</sub>N<sub>0.23</sub> (SRON)/SiO<sub>2</sub> bilayers were deposited on top of (100) Si substrate (*p*-type, base resistivity of 1–20  $\Omega$  cm) by means of plasma-enhanced chemical-vapor deposition. The SRON and SiO<sub>2</sub> layer thicknesses were kept constant at 4.5 nm and 1 nm, respectively. A subsequent high-temperature annealing treatment was carried out at 1150 °C for 1 h in N<sub>2</sub> ambient, to induce phase separation resulting in the excess Si precipitation and crystallization in the form of Si NCs, followed by H<sub>2</sub> defect passivation at 450 °C for 1 h. The material properties of analogous Si NC/SiO<sub>2</sub> MLs concerning NC size, crystalline quality and optical absorption and emission have been reported in the past.<sup>18–23</sup> Finally, a 200-nm-thick ZnO film was deposited by ALD at 200 °C (Refs. 15 and 16) and patterned by conventional photolithography, followed by full-area Al metallization of the rear side. A cross-section sketch of the studied devices is shown in the inset of Fig. 1. Further details on the multilayers deposition and device fabrication can be found elsewhere.<sup>7,24,25</sup>

Current-voltage [ $I(V)$ ] characterization was carried out in dark and at room temperature using an Agilent B1500 semiconductor device analyzer connected to a Microtech Summit 11000 probe station. Integrated electroluminescence was measured at room temperature by collecting the devices emission under DC electrical excitation with a Seiwa 888L

<sup>a)</sup>Electronic mail: julia.lopez.vidrier@imtek.uni-freiburg.de

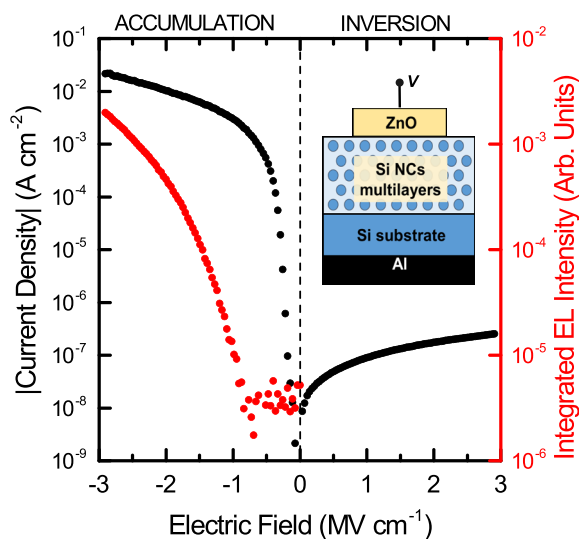


FIG. 1. Current density (black) and integrated EL emission intensity (red) as a function of the applied electric field. The inset shows a cross-section scheme of the devices under study.

microscope using a long working distance  $20\times$  objective ( $NA = 0.4$ ), coupled to a calibrated Hamamatsu GaAs R928 photomultiplier tube. The EL spectra were acquired by a Princeton Instruments LN<sub>2</sub>-cooled CCD coupled to a monochromator, under either DC or pulsed excitation. Time-resolved EL measurements were performed by collecting the resulting integrated EL emission using a high-time resolution Agilent Infiniium DSO 8064A oscilloscope.

The current density vs. electric field [ $J(E)$ ] characteristic of the device is presented in Fig. 1. As expected from the device design, the  $J(E)$  curve exhibits a strong rectifying behavior. At substrate accumulation ( $E < 0$ ) bipolar injection is possible, whereas in substrate inversion ( $E > 0$ ), the current is strongly limited by the  $p$ -Si depletion layer. Integrated EL intensity (red curve in Fig. 1) was measured over the whole scanned voltage range, although the actual signal was observed only in accumulation (see Ref. 8 for a detailed study on the power efficiency from devices containing analogous MLs). The onset for EL was found to be remarkably low, around  $-0.84 \text{ MV cm}^{-1}$  ( $\sim -2.3 \text{ V}$ ), corresponding to a minimum injection current density of  $\sim 10^{-3} \text{ A cm}^{-2}$  required to excite the luminescent centers within the device. This onset voltage is indeed comparable to previous reported works on similar structures.<sup>6</sup>

A further inspection of the EL emission properties of the device was performed by spectrally resolving the acquired signal, under a constant DC excitation of  $-7 \text{ V}$  (accumulation, equivalent to  $-2.55 \text{ MV cm}^{-1}$  and corresponding to  $J \sim 2 \times 10^{-2} \text{ A cm}^{-2}$ ). The resulting spectrum is displayed in Fig. 2(a), which exhibits a broad lineshape ranging from 400 nm to 1100 nm. Indeed, all acquired spectra could be deconvolved into two well-defined contributions, as observed in Fig. 2(a), peaking around 700 nm and 850 nm. The origin of the low-energy contribution is typically ascribed to the excitonic recombination at the fundamental quantum-confined electronic states of Si NCs.<sup>26</sup> For the sake of direct comparison, Fig. 2(b) presents an EL spectrum from a previous publication, corresponding to a Si NC MLs-based sample with the

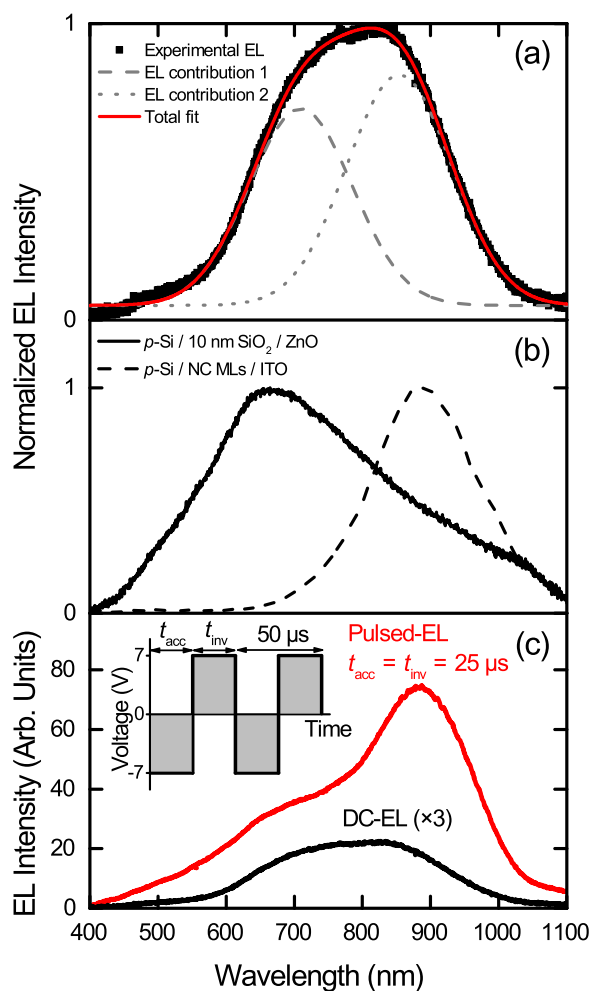


FIG. 2. (a) Normalized experimental EL spectrum acquired from the device under study (black points), fitted according to two different contributions (dashed and dotted grey lines), whose sum (solid red line) is in excellent agreement with the experimental data. (b) Normalized EL spectra corresponding to a reference sample containing a 10-nm-thick SiO<sub>2</sub> layer instead of NC MLs and ZnO electrode (solid line) and to an analogous NC ML sample (with ITO instead of ZnO as top electrode, dashed line) taken from Ref. 7. (c) Direct comparison between spectra acquired under DC (black) and pulsed (red) excitation. The inset shows the pulse schematics.

same structural parameters but with ITO instead of ZnO as top TCO electrode.<sup>7</sup> In fact, the fundamental difference between both samples, i.e., the different TCO, highlights the possibility that the high-energy EL contribution in Fig. 2(a) is related to ZnO. Again, Fig. 2(b) may shed light to the origin of this contribution by displaying the EL spectrum acquired on a reference sample containing a 10-nm-thick SiO<sub>2</sub> layer instead of Si NC MLs and with the same ALD-deposited ZnO on top. Note that in this case larger electric fields are required to achieve permanent current flow in the Fowler-Nordheim regime. This emission is centered around 700 nm, and its broadness indicates the excitation of luminescent centers within a wide range of electronic level energies, as usually obtained from deep-level defect states in ZnO (donor-acceptor pairs generated by O vacancies and Zn interstitials);<sup>27</sup> the fact that no near-band gap excitonic recombination of ZnO is observed around 380 nm (and thus no emission tail is detected)<sup>28</sup> can be due either to a lower excitation energy than the ZnO band gap or to no additional annealing treatment being carried out on the ZnO-deposited samples.<sup>17</sup> Actually,

the hypothesis of emission coming from ZnO intra-band gap defect states is supported by the observation of ZnO-related contribution broadening towards higher energies when increasing the DC excitation current density (not shown here), which promotes electron-hole pair generation in higher-energy defect states within the ZnO band gap.

Once the different contributions to EL were identified, efforts were focused on the effect of pulsed excitation on the emission. For this, a square voltage pulse, symmetric between  $-7$  V and  $7$  V (well within the accumulation and the substrate inversion regimes, respectively), was employed [see inset of Fig. 2(c)], whose result is displayed in Fig. 2(c) in comparison to the spectrum resulting from DC excitation at  $-7$  V [see Fig. 2(a)]. A pulse period of  $50$   $\mu$ s was selected (equivalent to a driving frequency of  $20$  kHz), which showed the maximum emission yield in our samples, in good agreement with previous reported works on analogous systems and methodologies.<sup>9,10,13</sup> In addition, we selected a 50% duty cycle, i.e., accumulation ( $t_{\text{acc}}$ ) and inversion ( $t_{\text{inv}}$ ) pulse times of  $25$   $\mu$ s, as schematized in the inset of Fig. 2(c). We observe a huge enhancement of the EL intensity under applied pulsed excitation, estimated as a factor  $\sim 9$  from the ratio between the EL integrated areas. This behavior was first observed by Walters *et al.*<sup>9</sup> and was attributed to the sequential injection of carriers from the Si substrate towards the active layer under alternate accumulation and inversion cycles. Provided that the system response to this type of excitation is tightly related to the carrier injection characteristics, the duty cycle of the pulse is expected to play an important role on the EL emission of the system. Under this assumption, we modified the duty cycle by applying different accumulation and inversion times, while keeping fixed the  $50$ - $\mu$ s pulse period. The limiting cases are displayed in Fig. 3. As can be observed, the spectral lineshape drastically evolves, shorter  $t_{\text{acc}}$  (and thus longer  $t_{\text{inv}}$ ) inducing the progressive quenching of the ZnO defects-related contribution, and consequently leaving Si NCs as the only active luminescent centers.

To understand the effect of the different pulsed excitation characteristics on the EL emission output, it is necessary to analyze the recombination dynamics taking place within the system. Fig. 4(a) displays the EL emission dynamics on a whole excitation period of  $1$  ms ( $t_{\text{acc}} = t_{\text{inv}} = 500$   $\mu$ s). This period was intentionally selected to provide complete charging of the luminescent species and corresponding EL decay. Please note that, since radiative recombination in ZnO defects emission typically takes place in the nanosecond range,<sup>29</sup> the observed slow EL decay in the figure (microsecond range) must necessarily be dominated by processes taking place within the Si NC MLs. Indeed, the dynamics pattern is similar to the ones reported in Ref. 8, where analogous Si NC MLs-based devices were analyzed that contained ITO electrode instead of ZnO, again evidencing that processes taking place in ZnO are not reflected in the observed dynamics. Focusing again on Fig. 4(a), markedly different phenomena occur under opposite charging regimes. In accumulation, EL emission increases up to a constant DC-like emission level, being the rise time estimated as  $\sim 18$   $\mu$ s. Once the pulse voltage is switched from  $-7$  V to  $7$  V, i.e., the deep depletion regime is reached, an EL overshoot (rise

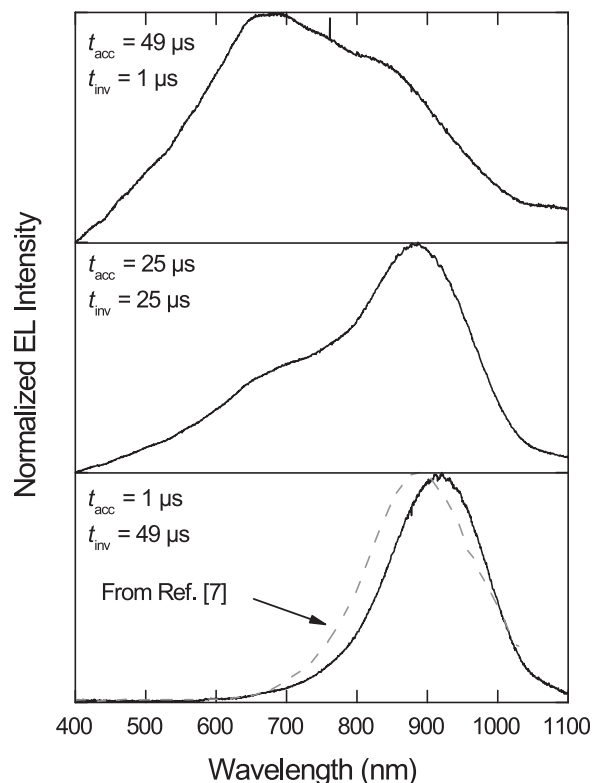


FIG. 3. Normalized EL spectra acquired under pulsed excitation, using a symmetric square-voltage pulse of  $-7$  V/ $7$  V and different accumulation and inversion times, while holding a fixed period of  $50$   $\mu$ s. The EL spectrum from an analogous sample from Ref. 7 is also displayed (grey dashed line).

time  $\sim 17$   $\mu$ s) takes place followed by a slow decay, whose single-exponential fit resulted in a decay time of  $\sim 76$   $\mu$ s. The estimated characteristic times are in good agreement with expected values for Si NCs.<sup>30–32</sup>

The EL recombination dynamics of the system sheds light on the carrier injection and excitation processes taking place within the device structure. These mechanisms are illustrated by the energy band diagrams displayed in Fig. 4(b). In accumulation, holes are injected into the Si NC MLs from the valence band of the  $p$ -type Si substrate, while electrons are injected from the ZnO top electrode. The observed emission of ZnO can only be explained by electron-hole generation as a consequence of hole injection from the Si NC MLs into the ZnO electrode, where a high concentration of electrons exists ( $\sim 5 \times 10^{19}$   $\text{cm}^{-3}$ ). Due to the large band offset between the ZnO and the Si NCs valence bands, ZnO is essentially a hole-blocking contact. However, defects-related deep-level states are possibly excited by holes, which is the reason of the missing observation of ZnO band gap transition in the EL spectra. Regarding the observed Si NCs-related EL emission, it must be a consequence of electron-hole pair generation within the quantum-confined NC states. Note that, because of injection asymmetry between electrons and holes (hole mobility is several orders of magnitude lower than that of electrons),<sup>33</sup> and although bipolar excitation of opposite electrode-injected carriers cannot be entirely ruled out, generation of electron-hole pairs in Si NCs most likely occurs via electron impact of tunneling electrons from the ZnO electrode.<sup>34</sup> However, it was recently shown that defect states at Si NC interfaces may allow for band-to-band

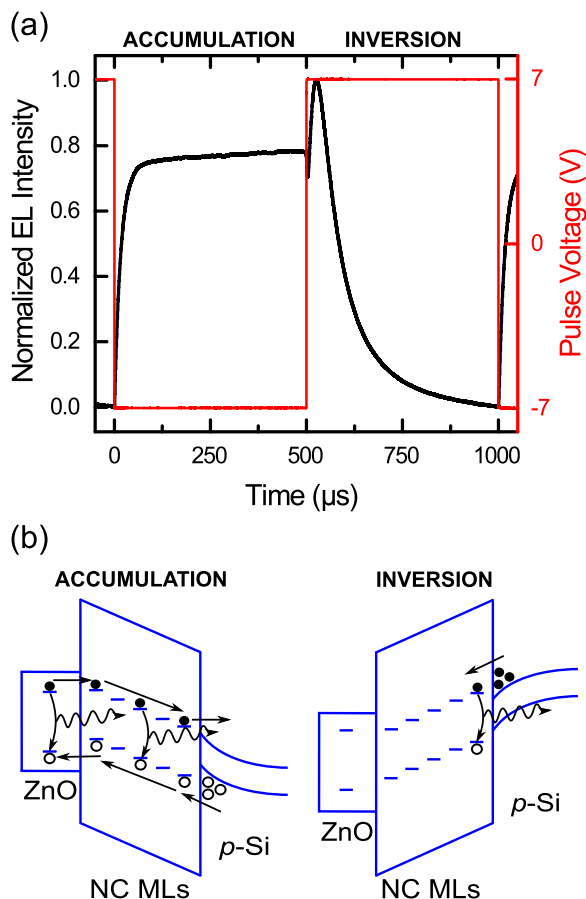


FIG. 4. (a) EL emission dynamics (black) over a period of 1 ms (50% duty cycle), corresponding to the device under study (the employed voltage pulse in red). (b) Energy band diagrams corresponding to the ZnO/NC MLs/*p*-Si system under the respective conduction regimes.

excitation at electric fields below  $1 \text{ MV cm}^{-1}$ ,<sup>25</sup> effectively generating massive amounts of holes that accumulate at the ZnO-MLs interface (mechanism not shown in the band diagrams). Both mechanisms are feasible in the present structure, and support the observed constant EL emission level. In this process, hole injection and defect-related hole generation within the Si NC MLs, as well as the higher electron mobility leading to more efficient electron transport through the MLs, may result in non-compensated (i.e., non-recombined) positively charged Si NCs. Under inversion, minority carriers from the substrate (electrons in the formed inversion layer at the substrate-MLs interface) are injected into these positively charged NCs via Coulomb field-enhanced tunneling, the so-called sequential carrier injection,<sup>9,10</sup> which induces electron-hole pair formation resulting in the EL emission overshoot observed in Fig. 4(a). This exciton formation is maximized when all positively charged NCs are neutralized, after which EL decays. Under this regime, excitation of the luminescent centers is not achieved because of both the unlikely hole injection from ZnO (*n*-type) and the low electron injection rate from the *p*-type substrate, so that neither bipolar nor impact excitation are possible; as a consequence, no EL emission is observed in conventional (DC-excited) spectra.

Recovering again the results displayed in Fig. 3, the proposed frame for excitation may explain the quenching of ZnO defects-related emission. When the pulse is governed

by the accumulation regime (i.e., longer  $t_{\text{acc}}$  is employed), hole injection into ZnO defects and electron impact of (or electron-hole bipolar injection into) Si NCs are achieved. In this case,  $t_{\text{inv}} = 1 \mu\text{s}$  is notably shorter than the inversion decay time ( $\sim 76 \mu\text{s}$ ), and thus complete discharge of the Si NCs is not fulfilled. As  $t_{\text{inv}}$  increases, exciton generation within ZnO and Si NCs still takes place, whereas the efficiency of Coulomb field-enhanced electron-hole pair formation is increased; this is translated into an enhancement of the Si NC-related EL with respect to ZnO. These findings are further supported by an enhanced Si NC-related EL emission observed when increasing the inversion voltage (not shown), where a more efficient electron injection from the inversion layer is achieved. Finally, when decreasing  $t_{\text{acc}}$  to  $1 \mu\text{s}$ , electron and hole injection is not efficient throughout the device, and thus no holes can be injected from the MLs into ZnO, which totally quenches ZnO emission. In contrast, this accumulation time is long enough to positively charge the Si NCs next to the substrate-ML interface, which favors recombination by neutralization within this region and results in the sole presence of Si NCs-related emission in the acquired spectra.

So far, this work has revealed that, in ZnO/Si NC MLs/*p*-Si LEDs, EL emission results from a complex charge injection and excitation pattern. On one hand, DC excitation in accumulation regime leads to emission by impact excitation of Si NCs and by electron-hole pair generation in ZnO after hole injection into deep-level intra-band gap defects. On the other hand, the recombination dynamics becomes far less intuitive when a pulsed excitation is employed, where a sequential Coulomb field-enhanced electron-hole generation adds to impact excitation, resulting in an enhanced EL emission with respect to the DC case. In addition, the relative emission from the different luminescent centers can be modified by controlling the pulse parameters ( $t_{\text{acc}}$  and  $t_{\text{inv}}$ ), which can be exploited towards particular optoelectronic applications requiring whole-visible range emission. Overall, these observations shed light to the sequential charging of Si NCs, a promising field for Si NCs EL. It is foreseen that the modification of NC-based LED design will lead to enhanced sequential bipolar excitation in detriment to inefficient impact ionization, which will notably improve the performance of Si NC-based devices.

This work was financially supported by the German Research Foundation (ZA191/27-3 and ZA191/33-1) and the Spanish Ministry of Economy and Competitiveness (TEC2016-76849-C2-1-R).

<sup>1</sup>L. T. Canham, *Appl. Phys. Lett.* **57**, 1046 (1990).

<sup>2</sup>F. Iacona, G. Franzò, and C. Spinella, *J. Appl. Phys.* **87**, 1295 (2000).

<sup>3</sup>F. Iacona, G. Franzò, V. Vinciguerra, A. Irrera, and F. Priolo, *Opt. Mater.* **17**, 51 (2001).

<sup>4</sup>M. Zacharias, J. Heitmann, R. Scholz, U. Kahler, M. Schmidt, and J. Bläsing, *Appl. Phys. Lett.* **80**, 661 (2002).

<sup>5</sup>A. Marconi, A. Anopchenko, M. Wang, G. Pucker, P. Bellutti, and L. Pavesi, *Appl. Phys. Lett.* **94**, 221110 (2009).

<sup>6</sup>A. Anopchenko, A. Marconi, E. Moser, S. Prezioso, M. Wang, L. Pavesi, G. Pucker, and P. Bellutti, *J. Appl. Phys.* **106**, 033104 (2009).

<sup>7</sup>J. López-Vidrier, Y. Berencén, S. Hernández, O. Blázquez, S. Gutsch, J. Laube, D. Hiller, P. Löper, M. Schnabel, S. Janz, M. Zacharias, and B. Garrido, *J. Appl. Phys.* **114**, 163701 (2013).

- <sup>8</sup>J. López-Vidrier, Y. Berencén, S. Hernández, B. Mundet, S. Gutsch, J. Laube, D. Hiller, P. Löper, M. Schnabel, S. Janz, M. Zacharias, and B. Garrido, *Nanotechnology* **26**, 185704 (2015).
- <sup>9</sup>R. J. Walters, G. I. Bourianoff, and H. A. Atwater, *Nat. Mater.* **4**, 143 (2005).
- <sup>10</sup>R. J. Walters, J. Carreras, T. Feng, L. D. Bell, and H. A. Atwater, *IEEE J. Sel. Top. Quantum Electron.* **12**, 1647 (2006).
- <sup>11</sup>M. Perálvarez, C. García, M. López, B. Garrido, J. Barreto, C. Domínguez, and J. A. Rodríguez, *Appl. Phys. Lett.* **89**, 051112 (2006).
- <sup>12</sup>J. Barreto, M. Perálvarez, J. A. Rodríguez, A. Morales, M. Riera, M. López, B. Garrido, L. Lechuga, and C. Domínguez, *Physica E* **38**, 193 (2007).
- <sup>13</sup>T. Creazzo, B. Redding, E. Marchena, J. Murakowski, and D. W. Prather, *Opt. Express* **18**, 10924 (2010).
- <sup>14</sup>O. Blázquez, J. López-Vidrier, S. Hernández, J. Montserrat, and B. Garrido, *Energy Procedia* **44**, 145 (2014).
- <sup>15</sup>J. Laube, D. Nübling, H. Beh, S. Gutsch, D. Hiller, and M. Zacharias, *Thin Solid Films* **603**, 377 (2016).
- <sup>16</sup>H. Beh, D. Hiller, J. Laube, S. Gutsch, and M. Zacharias, *J. Vac. Sci. Technol. A* **35**, 01B127 (2017).
- <sup>17</sup>R. Könenkamp, R. C. Word, and M. Godinez, *Nano Lett.* **5**, 2005 (2005).
- <sup>18</sup>S. Gutsch, D. Hiller, J. Laube, M. Zacharias, and C. Kübel, *Beilstein J. Nanotechnol.* **6**, 964 (2015).
- <sup>19</sup>J. López-Vidrier, S. Hernández, D. Hiller, S. Gutsch, L. López-Conesa, S. Estradé, F. Peiró, M. Zacharias, and B. Garrido, *J. Appl. Phys.* **116**, 133505 (2014).
- <sup>20</sup>H. Gnaser, S. Gutsch, M. Wahl, R. Schiller, M. Kopnarski, D. Hiller, and M. Zacharias, *J. Appl. Phys.* **115**, 034304 (2014).
- <sup>21</sup>S. Hernández, J. López-Vidrier, L. López-Conesa, D. Hiller, S. Gutsch, J. Ibáñez, S. Estradé, F. Peiró, M. Zacharias, and B. Garrido, *J. Appl. Phys.* **115**, 203504 (2014).
- <sup>22</sup>J. Valenta, M. Greben, Z. Remeš, S. Gutsch, D. Hiller, and M. Zacharias, *Appl. Phys. Lett.* **108**, 023102 (2016).
- <sup>23</sup>J. Ibáñez, S. Hernández, J. López-Vidrier, D. Hiller, S. Gutsch, M. Zacharias, A. Segura, J. Valenta, and B. Garrido, *Phys. Rev. B* **92**, 035432 (2015).
- <sup>24</sup>A. M. Hartel, D. Hiller, S. Gutsch, P. Löper, S. Estradé, F. Peiró, B. Garrido, and M. Zacharias, *Thin Solid Films* **520**, 121 (2011).
- <sup>25</sup>S. Gutsch, J. Laube, A. M. Hartel, D. Hiller, N. Zakharov, P. Werner, and M. Zacharias, *J. Appl. Phys.* **113**, 133703 (2013).
- <sup>26</sup>J. Valenta, N. Lalic, and J. Linnros, *Opt. Mater.* **17**, 45 (2001).
- <sup>27</sup>Y. Chen, D. M. Bagnall, H. Koh, K. Park, K. Hiraga, Z. Zhu, and T. Yao, *J. Appl. Phys.* **84**, 3912 (1998).
- <sup>28</sup>Y. X. Liu, Y. C. Liu, C. L. Shao, and R. Mu, *J. Phys. D: Appl. Phys.* **37**, 3025 (2004).
- <sup>29</sup>A. J. Morfa, B. C. Gibson, M. Karg, T. J. Karle, A. D. Greentree, P. Mulvaney, and S. Tomljenovic-Hanic, *Nano Lett.* **12**, 949 (2012).
- <sup>30</sup>N. Lalic and J. Linnros, *J. Appl. Phys.* **80**, 5971 (1996).
- <sup>31</sup>J. Linnros, N. Lalic, A. Galeckas, and V. Grivickas, *J. Appl. Phys.* **86**, 6128 (1999).
- <sup>32</sup>M. Dovrat, Y. Goshen, J. Jedrzejewski, I. Balberg, and A. Sa'ar, *Phys. Rev. B* **69**, 155311 (2004).
- <sup>33</sup>J. F. Verwey, E. A. Amerasekera, and J. Bisschop, *Rep. Prog. Phys.* **53**, 1297 (1990).
- <sup>34</sup>Z. Liu, J. Huang, P. C. Joshi, A. T. Voutsas, J. Hartzell, F. Capasso, and J. Bao, *Appl. Phys. Lett.* **97**, 071112 (2010).